A Model for Electrochromic Tungstic Oxide Microstructure and Degradation

A Model for Electrochromic Tungstic Oxide Microstructure and Degradation

Thomas C. Arnoldussen*[,1]

General Motors Research Laboratories, Electronics Department, Warren, Michigan 48090

ABSTRACT

Despite much investigation of the electrochromic (EC) coloration process in WO_3 films, such displays have not yet become commercially viable because of limited useful device life. Device degradation occurs by WO_3 film dissolution on the shelf and erosion during cycling. Water plays a crucial role in both efficient coloring/bleaching and in film degradation. To better understand the degradation process and the role of water, dissolution of EC WO_3 films in aqueous media was studied. The results strongly suggest that EC films formed by evaporation are amorphous molecular solids consisting of trimeric W_3O_9 molecules bound weakly to each other through water-bridge, hydrogen, and van der Waal's bonding. The nature of this microstructure is responsible for the high solubility. Films subjected to ion bombardment show decreased dissolution rates as well as decreased electrochromism and, while amorphous, are believed to have a random network rather than molecular microstructure.

The chief problem to be overcome before electrochromic displays can be commercially viable is the short device life. Degradation of WO_3-acid electrolyte ECD's is associated with film dissolution on the shelf and erosion during cycling. Aqueous acid cells show superior performance from the standpoint of response speed, however, water is a primary culprit in shortening lifetimes through WO_3 dissolution. Nevertheless, Knowles and Hersh have shown (1) that some water must be incorporated in the WO_3 film, even in so-called "aprotic" devices to obtain any electrochromic coloration. Others have studied WO_3 in aprotic solvents but have not systematically analyzed their films for water content as have Knowles and Hersh. The need to better understand the role of water in electrochromism, the interaction of H_2O and WO_3, and the mechanism of ECD degradation have motivated the work presented here. Study of WO_3 dissolution is a proper starting point and provides several key insights into the nature of electrochromic films and the electrochromic process. Others (2, 3) have reported data on dissolution rates of EC WO_3 films in various solvents, but have not related the high observed rates to a detailed physical mechanism or to the nature of the film itself.

Amorphous WO_3 Film Dissolution (Aqueous)

Theoretical.—The thermodynamic equilibrium between crystalline WO_3 and water predicts that WO_3 dissolves by hydrolysis to form normal tungstate ions, WO_4^{2-}, plus $2H^+$. The solubility at 25°C is 1.3×10^{-5} moles/liter in a neutral starting solution and decreases exponentially with decreasing *p*H. The presence of other species of tungstate ions is negligible. According to this result, a crystalline film 1 cm^2 in area exposed to 1 cm^3 water should saturate the solution after only 4.0 nm of film has dissolved. In an acid environment of *p*H ~1-2 such as used in EC devices, much less than one molecule-layer would dissolve. By comparison, an EC film which is amorphous and usually deposited by evaporation (0.5-1.0 μm thick) dissolves comparatively fast and completely, even in the small volumes of low *p*H solutions used in EC devices. We expect the somewhat higher free energy of an amorphous film to drive dissolution more strongly, but unless WO_4^{2-} ions precipitate from solution elsewhere as $WO_3 \cdot nH_2O$ or are converted to metastable polytungstate ions, saturation should ensue and dissolution cease.

Experimental observation during film dissolution indicates no evidence of reprecipitation as WO_3 particles for amorphous films dissolving completely in small volumes of DI water or acid solutions. This strongly suggests that amorphous WO_3 forms polytungstate anions (such as the metatungstate ion which is very stable even in strong acids) (3) upon dissolution. Dissolved WO_3 concentration can reach values far above that expected to produce precipitation. Only many days after a film has been dissolved, or upon extreme concentration of the solution by solvent evaporation, are precipitate particles observed. Crystalline WO_3 dissolves as normal tungstate (WO_4^{2-}) ions according to the hydrolysis reaction

$$WO_3(c) + H_2O \rightleftharpoons 2H^+ + WO_4^{2-}, \quad K_N = 10^{-14.05} \quad [1]$$

Tungstate ions are also known to agglomerate in acid solution to form polymeric anions (4) according to

$$7H^+ + 6WO_4^{2-} \rightleftharpoons HW_6O_{21}^{5-} + 3H_2O, \quad K_{PA} = 10^{53.98} \quad [2]$$

$$14H^+ + 12WO_4^{2-} \rightleftharpoons W_{12}O_{41}^{10-} + 7H_2O, \quad K_{PB} = 10^{110.03} \quad [3]$$

$$18H^+ + 12WO_4^{2-} \rightleftharpoons H_2W_{12}O_{40}^{6-} + 8H_2O, \quad K_M = 10^{132.51} \quad [4]$$

where the polyanions formed in Eq. [2]-[4] are called paratungstate A, paratungstate B, and metatungstate, and the various K's are molar equilibrium constants at 25°C. Pseudo-metatungstate ($HW_6O_{20}^{3-}$) may also be formed. When crystalline WO_3 is allowed to dissolve in an aqueous medium, each of these species can form. The H^+ concentration (C_H) is given by the charge balance

$$(C_H - C^o_H) - (C_{OH} - C^o_{OH}) = 2C_N + 5C_{PA} + 10C_{PB} + 6C_M \quad [5]$$

where the C's denote molar concentrations of the ions noted in Eq. [1]-[4].

C_{OH} is the hydroxyl ion concentration and C^o_H and C^o_{OH} refer to the H^+ and OH^- concentrations of the initial solvent before WO_3 dissolution has occurred. For dissolution in DI water, which is neutral-to-weakly acid, the C_{OH} and C^o_{OH} terms may be ignored. The total molar concentration of dissolved WO_3, C_W, is given by the mass balance

$$C_W = C_N + 6C_{PA} + 12C_{PB} + 12C_M \quad [6]$$

* Electrochemical Society Active Member.
[1] Present address: IBM, San Jose, California 95193.
Key words: electrochromic tungstic oxide, dissolution.

Equations [5] and [6] apply regardless of whether the solubility limit has been reached. Equation [5] applies only for dissolution of an oxide, not a tungstate salt, while Eq. [6] pertains to dissolved oxides or salts. The solubility of crystalline WO_3 may be determined using Eq. [5] and [6] in conjunction with the equilibrium mass action relations derived from Eq. [1]-[4]. Doing this, one finds that the solubility of crystalline WO_3 in water is 1.30×10^{-5} moles/liter and the pH attained at saturation is 4.58, corresponding to essentially all the dissolved WO_3 in the form of normal WO_4^{2-} ions. The author verified this pH and solubility experimentally.

A similar quasi-equilibrium analysis for dissolving amorphous WO_3 is unsuitable. This would require (*i*) that the kinetics of reprecipitation elsewhere as crystalline WO_3 be so slow as to be ignored for the time periods of interest, (*ii*) that the detailed mechanism of dissolution be the same as for crystalline WO_3 shown in Eq. [1], and (*iii*) that a dynamic microscopic quasi-equilibrium between the amorphous WO_3 surface and the solution tungstates exists. Experimental observation suggests that condition (*i*) may be met, but there is no evidence to justify assuming that conditions (*ii*) and (*iii*) hold.

Therefore we cannot predict the solubility of an amorphous WO_3 film. In fact, we cannot even say whether quasi-equilibrium solubility is a tenable concept for amorphous WO_3. However, we would expect the solution equilibria expressed by Eq. [2]-[4] to be obeyed regardless of the particular dissolution kinetics and thermodynamics. This permits us to use an indirect approach to investigate amorphous WO_3 dissolution, yet draw some important conclusions.

If we assume various values of dissolved WO_3 concentrations, C_W, then by means of Eq. [2]-[6] we can calculate the pH achieved as a result of dissolution and the distribution of tungsten among the various tungstate and polytungstate species when solution quasi-equilibrium is reached. The result of such a calculation is shown in Fig. 1, showing the quasi-equilibrium curves for pH and tungsten: (free) proton ratio as a function of C_W for dissolution in neutral water. The tungsten: proton ratio is a convenient representation of the distribution of tungsten among the various polytungstate species since this ratio is uniquely determined by the equilibrium distribution. For example, if all the tungsten were in the form of WO_4^{2-} ions, this ratio would be 1:2; if all were in the form of $H_2W_{12}O_{40}^{2-}$, this ratio would be 2:1.

Chemical processes generally do not proceed immediately to equilibrium (particularly true for the reactions considered here). If amorphous WO_3 dissolution proceeds as crystalline WO_3, one WO_3 unit at a time hydrolyzing to form one WO_4^{2-} ion plus two free H^+, we would expect that during and for sometime after dissolution, the pH and C_W: (C_H — C^o_H) ratio would be lower than the values given by the quasi-equilibrium curves of Fig. 1. There would be an excess of lower order species (monomeric ions) and free protons. During equilibration, the excess acidity would induce polymerization of the normal tungstate ions, thereby consuming protons and raising the pH and the C_W: (C_H — C^o_H) ratio. On the other hand, if after dissolving an amorphous film in water we found the measured pH and C_W: (C_H — C^o_H) ratio to fall on the high side of the quasi-equilibrium curves, we would be forced to conclude that the amorphous WO_3 entered solution directly in a polymerized form with equilibration proceeding in the direction of depolymerization.

Experimental

With these theoretical considerations in mind, the following experiment was performed. A 0.70 μm thick WO_3 film was evaporated onto an unheated glass substrate from a Ta boat. The film area was 2.5 cm^2. This film was placed in 40 ml DI water (pH = 6.15, slight acidity due to dissolved CO_2 presumably) and allowed to dissolve. When dissolution was complete, the pH was measured to be 4.35. This was lower than the 4.58 value predicted and measured for crystalline WO_3. This solution was then titrated back to neutrality while monitoring the pH. A pH = 11.65 NaOH titrant was used. The solution was constantly stirred and 5 min elapsed between each addition of NaOH and the pH measurement. The titration curve is shown in Fig. 2.

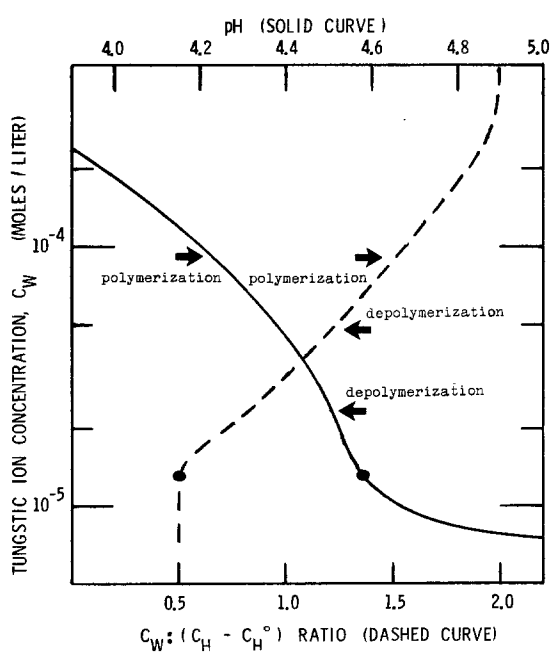

Fig. 1. Calculated quasi-equilibrium curves for pH and tungsten: free proton ratio, assuming various amounts of WO_3 to be dissolved by neutral H_2O. Measured values falling to the left or right of these curves imply equilibration occurs by polymerization or depolymerization, respectively. Dots on lower portions of curves correspond to crystalline WO_3.

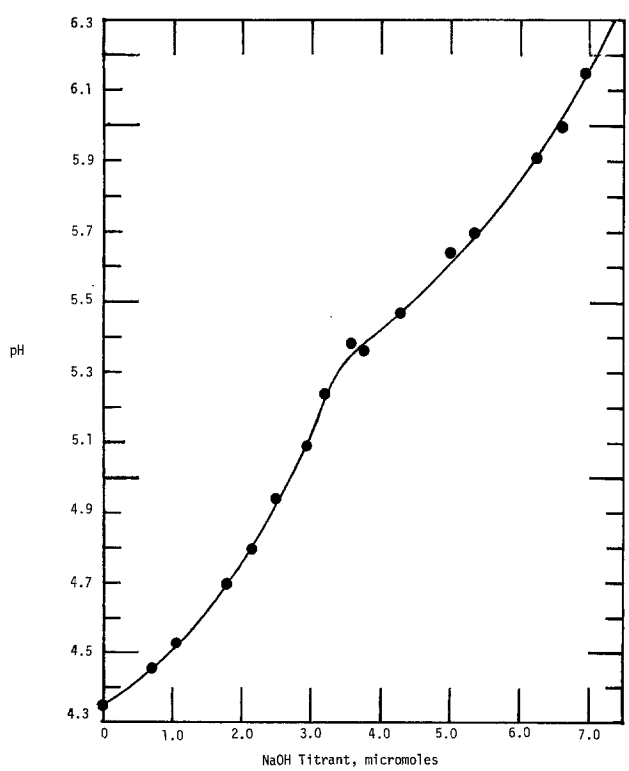

Fig. 2. Titration curve for amorphous WO_3 film dissolved in 40 ml DI water. Film was 2.5 cm^2 and 0.70 μm thick.

The features of interest here are the initial pH of the dissolved film solution, the quantity of NaOH added to return the pH to that of the DI water (pH = 6.15), and the appearance of a cusp at about 3.4×10^{-6} moles NaOH. From the initial pH = 4.35 of the dissolved film solution and the pH of the starting DI water, we calculate the H^+ concentration due to WO_3 film dissolution is $C_H - C^o_H = 4.40 \times 10^{-5}$ moles/liter. The cusp is characteristic of a depolymerization process induced by raising the pH.

At the point where the pH has been restored to that of the DI water used to dissolve the film, virtually all the WO_3 in solution may be assumed to be in the form of WO_4^{2-} ions and we have essentially a Na_2WO_4 salt solution. The quantity of NaOH needed to reach this point, $C_{Na} = 1.74 \times 10^{-4}$ moles/liter, gives the total concentration of tungsten ions in solution: $C_W = C_{Na}/2 = 8.71 \times 10^{-5}$ moles/liter. The ratio C_W: $(C_H - C^o_H)$ is 1.98:1. This is essentially the ratio (2:1) expected if WO_3 goes into solution from the amorphous film as metatungstate ions, $6H^+ + H_2W_{12}O_{40}^{6-}$. Pseudo-metatungstate, $3H^+ + HW_6O_{20}^{6-}$, could also be the species formed since the tungsten/proton ratio is likewise 2:1.

The important result here is that both the pH and the tungsten:free proton ratio resulting from the dissolution of this amorphous evaporated WO_3 film fall significantly to the high side of the quasi-equilibrium curves shown in Fig. 1. The amount of normal tungstate (WO_4^{2-}) present is less than 3% of that needed to maintain equilibrium with the metatungstate. Clearly, we must infer that the film dissolves not as WO_4^{2-} which subsequently polymerizes, but as 6- or 12-mer ions or as unstable 3-mer ions which quickly form metatungstate or pseudo-metatungstate. Any reactions going on in solution must be in the direction of depolymerization.

The titration results also allow us to calculate the film density from the measured C_W and film thickness and area. We obtain 1.20×10^{22} tungsten ions/cm³ or 4.62 g/cm³ assuming stoichiometric WO_3 free of water. Evaporated WO_3 has been reported (5) to contain as much as 0.5 H_2O per WO_3 which would increase the mass density to 4.80 g/cm³. These values compare with densities ~5 g/cm³ reported by Randin (2) using another technique.

Proposed Structural Model

One clue to understanding the high solubility of evaporated amorphous WO_3 and the peculiar way in which it dissolves directly as polytungstate ions is seen by examining the proposed structures of metatungstate and pseudo-metatungstate ions, shown in Fig. 3. The basic building block of polytungstate ions is a trigonal unit consisting of three edge-sharing WO_3 octahedra. The metatungstate ion (Fig. 3a) is formed by four such trigonal units tetrahedrally coordinated, sharing corners, about a central tetrahedral void containing two trapped protons (3). Similarly, a pseudo-metatungstate ion (Fig. 3b) may be formed by two such trigonal units sharing faces with one proton trapped in the central bi-pyramidal void.

This tendency to form trigonal or trimeric units reappears in numerous WO_3 related substances. Various forms of crystalline tungsten bronzes and solid tungstate salts also contain trigonally oriented octahedra forming low symmetry structures with 3, 5, and 6 member rings. Hashimoto *et al.* have shown that near sublimation temperature WO_3 forms a hexagonal phase (6). And the vapor generated by subliming WO_3 has been shown (7) to consist chiefly of trimeric W_3O_9 molecules as schematically shown in Fig. 4a. Such trigonal clustering may be attributed to formation of delocalized molecular orbitals within the three member ring stabilizing the structure.

The demise of an evaporated amorphous WO_3 film by dissolution as clusters of trigonal units provides

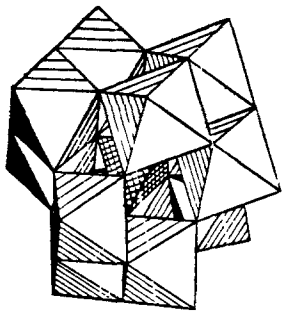

METATUNGSTATE $6H^+ + H_2W_{12}O_{40}^{6-}$

(a)

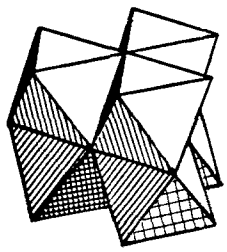

PSEUDO-METATUNGSTATE $3H^+ + HW_6O_{20}^{3-}$

(b)

Fig. 3. (a). Metatungstate ion composed of four tetrahedrally oriented trigonal units sharing corners with two protons in the center cage. Each trigonal unit consists of three edge-sharing WO_6 octahedra (4). (b). Pseudo-metatungstate ion is composed of two trigonal units sharing faces with one proton in the center bi-pyramidal void.

one clue to understanding the degradation process. The second important clue is obtained by examining the manner in which such a film is formed during vapor condensation.

As mentioned, the vapor generated by subliming WO_3 consists chiefly of trimeric W_3O_9 molecules illustrated in Fig. 4a. There is also a strong tendency for WO_3 to carry water of hydration, two possible forms of hydrated trimers being shown in Fig. 4b and 4c. When trimeric molecules are deposited at a high rate on low temperature substrates, such as in EC film deposition, it is probable that they remain more or less intact, bonding together weakly through van der Waal's forces or through water-bridge hydrogen bonding. Such phenomena have been observed in evaporation of elemental species such as sulfur and selenium and compounds such as As_2O_3. Evaporating As_2O_3 generates As_4O_6 vapor molecules which upon condensation form the metastable As_4O_6 molecular solid arsenolite (8, 9). Due to the relative stability of molecules exhibiting such associative tendencies, some activation energy is needed to dissociate them into the simplest molecular units before the lower energy network structure can form.

We expect the situation to be similar in EC film deposition, where insufficient thermal activation energy is available to dissociate trimers into monomers

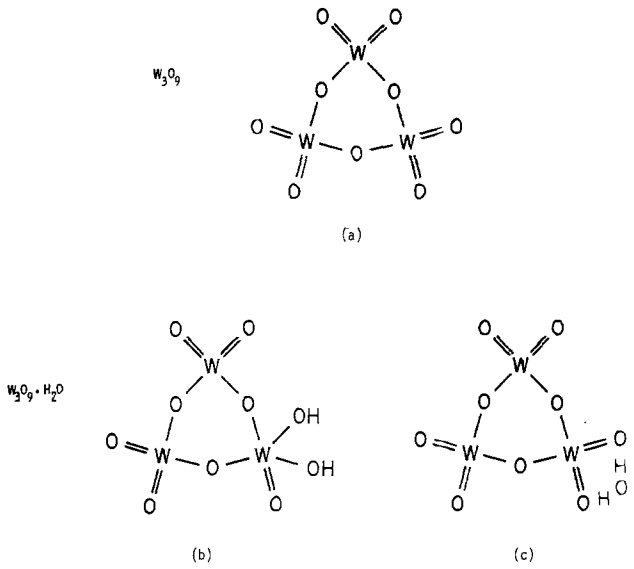

Fig. 4. (a). Schematic representation of W_3O_9 trimeric vapor molecule. (b) and (c). Two possible forms of monohydrated W_3O_9 molecule.

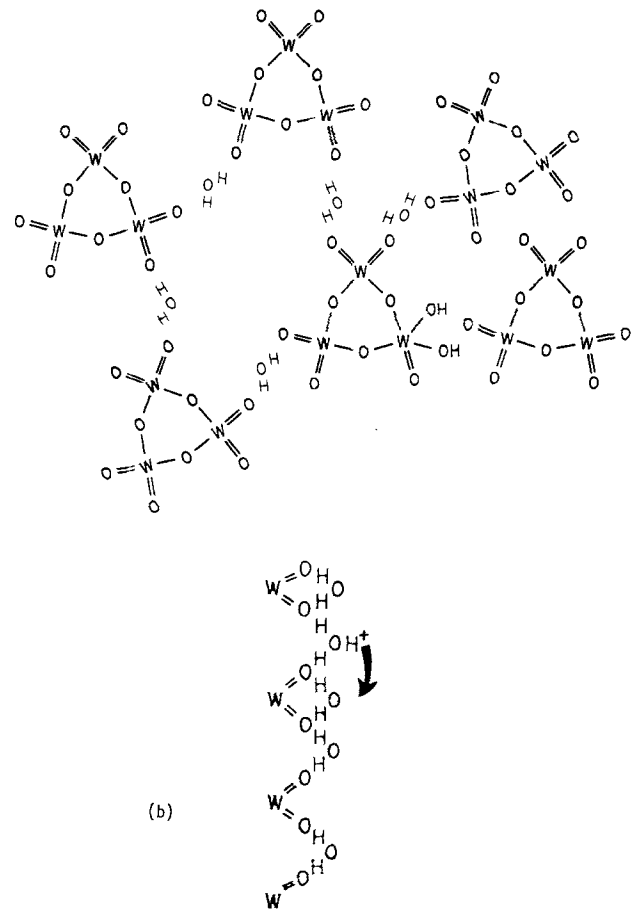

Fig. 5. (a). Representation of EC film as an amorphous molecular solid composed of W_3O_9 trimers banded together by water-bridge, hydrogen, and van der Waal's bonding. (b). Example of water molecule chain which can form giving rise to high proton mobility by H_3O^+ rotation and porton transfer to adjacent H_2O.

or to break the outer oxygen double bonds which is a precondition to network formation. Moreover, water of hydration, located at outer oxygens of the trimer, will further inhibit W-O-W cross bonding and network formation. Any inter-trimer bonding which does occur is likely to be weakened by lattice distortions inherent in an amorphous structure, while intra-trimer bonding should remain strong and largely unaffected by the disordered arrangement of trimeric units.

The picture that evolves is that an evaporated amorphous WO_3 film, as-deposited, resembles an amorphous molecular solid, rather than an amorphous random network structure, comprised of trimeric units bound weakly to one another such as depicted in Fig. 5. It is easy to imagine that when such a film is placed in an aqueous solution such trimers hydrolyze directly to the trigonal building blocks of polytungstate ions, without forming monomeric WO_4^{2-} ions as an intermediate step. This would account not only for the high solubility of such films, but also for the observation that they dissolve directly as polymeric ions. Trigonal ions carrying high coulombic charge can lower their free energy by agglomerating to form larger clusters of lower charge such as the metatungstate ion. This may occur on the dissolving surface or immediately after entering solution.

Film Restructuring

If evaporated amorphous WO_3 films are molecular solids as proposed then, if by some means one could break double bonds, perhaps even dissociate trimers, rebonding with neighboring molecules could occur to form a lower free energy network structure. Such a film should exhibit a decreased solubility compared to the as-deposited film. Raising the average lattice temperature (energy) by heating, as in recrystallization, is one way of dissociating the trimers. In this case, all the molecules are raised to an activated state simultaneously and can, therefore, undergo a cooperative rearrangement to form a crystalline network with considerable long range order. This would provide no further insight, since we already know that crystalline WO_3 has low solubility.

One can also induce lattice restructuring without crystallization by bombarding the sample with particles of sufficient energy. The activation energy thus provided is absorbed discontinuously in space and time without raising the average lattice temperature significantly. Crystallization would be inhibited because, at any given time, only individual molecules or very localized regions are in an activated state. Only short range restructuring or relaxation is expected. Amorphous WO_3 films were bombarded by implanting $10^{15}/cm^2$, 70 keV oxygen ions into the film. Primary energy transfer is by ion collisions with the lattice to a depth of 100-150 nm and secondary transfer is by high energy phonon or photon excitation ("thermal spikes") generated by collisions. The incident ion power was ~4 mW/cm^2 and the temperature rise was small, well below the recrystallization temperature of ~345°C (5).

Figure 6 shows an x-ray diffraction pattern obtained by using a rotating nanogram diffraction camera and particles of the bombarded film scraped from the substrate. Only amorphous-like halos are seen. One extends from about 0.24-0.48 nm and another faint halo is centered near 0.18 nm. These correspond to nearest W-W and W-O distances, respectively.

Such bombarded films, despite the implantation of oxygen, were slightly reduced as evidenced by a very slight bluish cast. A several hour postbake in air at 130°C (well below crystallization temperature) was sufficient to reoxidize the films to a transparent yellow. Virgin films used as control samples were given this same baking procedure to guarantee that any differences in film properties were due to the ion bombardment rather than thermal treatment.

As hypothesized, the bombarded films showed over an order of magnitude decrease in dissolution rate in neutral water compared to unbombarded films. They remained more soluble than crystalline WO_3, as might be expected for an amorphous structure. In aqueous acid solutions, bombarded films showed no evidence of significant dissolution even after many weeks in the

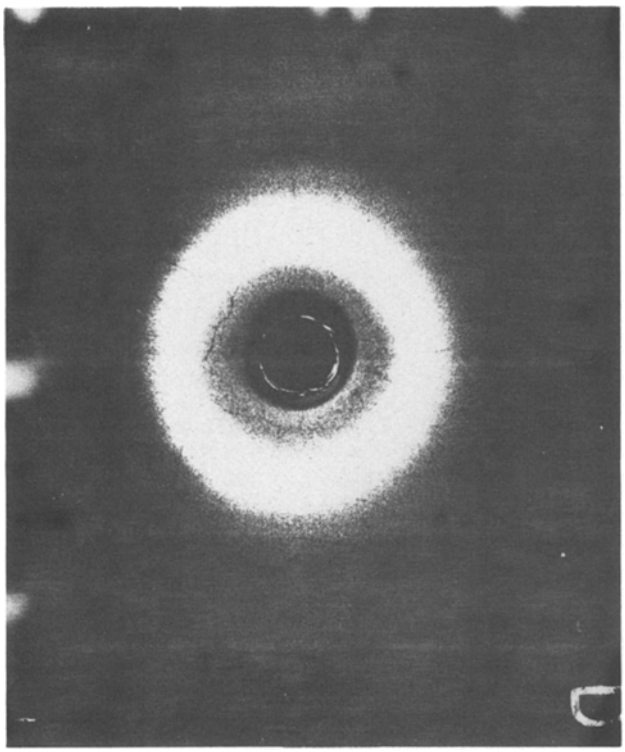

Fig. 6. Nanogram powder diffraction pattern for $10^{15}/cm^2$ 70 keV oxygen ion implanted WO_3 film. Pattern appears amorphous.

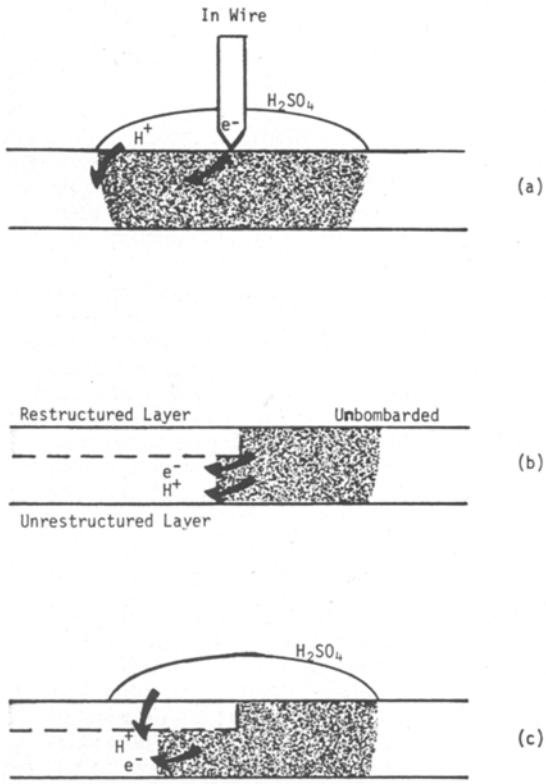

Fig. 7. (a). In wire/H_2SO_4 film coloration technique (10). In dissolves as In^{3+} causing $3e^- + 3H^+$ to be injected into the film. (b). Left portion of film partially restructured (upper layer) by ion bombardment. Right side colored by In/H_2SO_4, rinsed, and dried. Color bleeds slowly into region beneath restructured layer by lateral proton controlled $e^- + H^+$ diffusion. (c). Same as (b) but acid overlaps two regions. Color bleeds rapidly into region beneath restructured layer by lateral electron diffusion plus proton flow through restructured layer.

solvent, whereas virgin films dissolve within one to several days. This dramatic change in solubility is strong evidence of a change in local bonding and microstructure, and it suggests that WO_3 may indeed exist in two distinct amorphous forms: an amorphous molecular solid and an amorphous random network. In addition to the solubility change, ion bombardment produces the additional effect of destroying (or greatly decreasing) the electrochromism.

Electrochromic WO_3 films were also subjected to low energy ion/electron bombardment in an rf glow discharge chamber used for photoresist ashing (~13 Pa O_2, 13.56 MHz, 75W rf power capacitively coupled into a cylindrical chamber 7.6 cm in diameter and 15 cm deep with 50Ω impedance). Again, little heating occurred. Unlike the ion implantation bombardment, the electron/ion energies were only of order 10 eV. Similar decrease in solubility was observed for such low energy bombardment. While it has not been ruled out, chemical oxidation effects are not believed to be responsible for the solubility change. The low energy bombarded films showed no signs of reduction, as did the high energy implanted films (bluish cast), and may in fact have undergone some additional oxidation. Yet both types of bombardment produced the same solubility and colorability change.

Colorability of these bombarded films was checked by the indium wire/H_2SO_4 technique (10). This involves placing an acid droplet on the film and touching an In wire to the surface through the droplet. In dissolves as In^{3+} and the excess electrons on the wire are injected into the film. $3H^+$ are displaced from solution by the In^{3+}, entering the film to neutralize the injected electrons. The coloration spreads from the In contact radially (see Fig. 7a).

In the case of low energy bombardment, the colorability through the surface decreases rapidly during the first 5-10 min of bombardment, but lateral "color bleeding" from an adjacent unbombarded region remains possible until 20-30 min of bombardment have elapsed. This suggests a restructuring process which begins at the upper surface and migrates to the substrate with continued bombardment. (X-ray diffraction was done on 30 min bombarded films.)

In the coloration tests on samples bombarded for 5-10 min, if an unbombarded region is colored up to the boundary with a bombarded region and the sample is rinsed and dried, diffusion of color into the bombarded region is slow (~0.1 mm in ½ hr). If the acid droplet is not removed and overlaps the two regions, color diffusion is rapid (~0.5 mm/sec). These observations are essentially the same as for an unbombarded film, slow color diffusion in the absence and fast diffusion in the presence of an electrolyte. The difference is that an unbombarded film colors by direct contact of the In wire (through an acid) to the film surface, while the bombarded film does not. Moreover, an unbombarded film, so colored, can be bleached thoroughly by heating in air at 135°C for 15-30 min. A bombarded film, colored by bleeding from an unbombarded region, does not bleach even after days of heating in air.

These results may be interpreted as follows. Low energy bombardment restructures the upper portion of the film, leaving the lower portion unchanged (for bombarding times $\lesssim$ 10 min). Color bleeds from an unbombarded region into the deeper layer of the bombarded region. In the absence of an electrolyte on the surface, this proceeds by lateral diffusion of electrons and protons from the unbombarded region and is proton diffusion controlled. See Fig. 7b. In the presence of the acid on the surface, the fast color diffusion must be interpreted as lateral diffusion of electrons from the unbombarded region coupled with proton diffusion through the bombarded surface to neutralize the electrons (10). See Fig. 7c. The high speed of color diffusion cannot be explained by lateral proton diffusion.

The inability to color the bombarded region directly by In wire contact, the fast lateral bleeding, and the inability to bleach such a region, once colored by lateral bleeding, implies that the bombarded, restructured layer is still proton permeable, but is blocking to electron transport. The restructuring strengthens the overall bonding (evidenced by decreased solubility) without significantly diminishing the fast proton transport. But it apparently does inhibit electron injection or transport, or induces noncoloring trapping states.

These bombardment studies suggest two important concepts which are worth further investigation: (*i*) It may be proper to speak of not one amorphous state for WO_3, but two: one being closer to a molecular solid, the other a random network. Only the former is electrochromic. (*ii*) Lattice porosity and incorporated H_2O giving high proton mobility may be necessary but insufficient to produce rapid electrochromic response. The electronic states produced by a particular structure are of critical importance to electrochromic response.

Nonaqueous Solvents

It is apparent that EC device shelf degradation in aqueous electrolytes is caused by polytungstate formation. The much lower solubility of EC films in organic solvents may be understood in terms of solvent ionizability, solvent molecule size, and the nature of the solute ion formed. Dissolution is favorable when W-O-W bonds are broken in such a way that the bonds remain saturated. Water is a particularly good solvent because its small size permits it to attack a W-O-W bond and form two saturated W-OH HO-W bonds with a small local distortion of the lattice. Upon going into solution, $(WO_3)_n$ combines with water to form the compact tungstate and polytungstate ion structures. On the other hand, solvents which are not ionizable show little if any action on WO_3 films. Alcohols and glycols with one or more OH radical may ionize to form $R^+ + OH^-$ or $RO^- + H^+$ but are poor solvents for WO_3 films because (*i*) they do not ionize as readily as water, (*ii*) their molecular size is too bulky to penetrate the lattice without severe lattice distortion, and (*iii*) the R^+ and RO^- radicals are too bulky to form compact or complex polytungstate ions in solution. Dissolution in these solvents is likely to be limited to molecular species or simple monomeric ions. Solubility should be low in either case. When an electrolyte, such as H_2SO_4, is added to a nonaqueous solvent, an additional dissolution mechanism may be operative, namely, formation of electrolyte anion-WO_3 complexes. This is further discussed in the next section.

Cycling Degradation

EC device cycling degradation in aqueous and nonaqueous acid electrolytes occurs by an erosion process, probably similar to dissolution, but enhanced by the voltage drive. Film thinning during cycling has been measured by optical interference techniques (2). In aqueous electrolytes, the quiescent dissolution process occurs by polytungstate ion formation and diffusion into the electrolyte. Intuitively, one might expect that it is the nonequilibrium nature of the color/bleach process which leads to cycling degradation. However, nonequilibrium by itself does not imply degradation. A more detailed model is needed. In the literature it has frequently been suggested that cycling degradation may be due to such things as impurities or "irreversible side reactions." Having delineated the nature of quiescent dissolution of electrochromic WO_3 films in the present work, we propose the following intrinsic mechanism of cycling degradation.

In the bleached or moderately colored quiescent state, the electrode potentials are such that the Helmholtz double layer probably has the following structure. The inner layer consists of (*i*) a monolayer of chemisorbed H_2O forming a surface layer of tungstic-oxide-hydroxide which is anionic in nature; (*ii*) just beyond the surface is a layer of predominantly electrolyte anions plus polytungstate anions. The outer layer is chiefly $H_2O + H_3O^+ +$ protons with hydration shells of six or more water molecules. During the coloration cycle, electrolyte and polytungstate anions are driven away from the surface by the applied voltage, while hydrated protons are driven toward it. During this disturbance of the Helmholtz double layer, the depletion of polytungstate anions leads to the removal of tungstic oxide-hydroxide surface molecules to replenish polytungstate anions in the double layer. At the same time, the hydrated protons shed much, if not all, of their water of hydration upon entering the WO_3 surface, leaving an abundance of bond-breaking water molecules in the surface region and inner Helmholtz layer, further promoting dissolution.

While the current carried by the negative tungstate ions leaving the surface may be a small fraction of the proton current, over thousands of cycles it is sufficient to completely erode the film. This voltage-enhanced dissolution would account for the device cycle life decreasing with increased switching speed (higher voltage drive, greater anion depletion, and greater disturbance of the double layer structure) and with increased final point coloration (increased total charge driven per cycle). We expect and, in fact, observe that fast switching to a low contrast state produces more degradation per cycle than slow switching to a high contrast state.

Voltage-enhanced dissolution in nonaqueous electrolytes may occur by one of the following mechanisms. Dissolution by tungstate ion formation requires an oxygen donor species such as H_2O. If there were no dissolved oxygen or trace water in the electrolyte/solvent, and if neither the electrolyte nor solvent dissociate or electrolyze to donate oxygen, tungstate ions cannot form by interaction with the electrolyte. H_2O incorporated in the WO_3 during deposition could, however, contribute to tungstate formation. The H_2O:WO_3 ratio can be as high as 1:2 in evaporated films (5) while to form metatungstic acid only 1:3 is needed. Thus, the water incorporated in the film, apparently necessary to achieve high cation mobility (1), may be a self-contained cause of cycling degradation. In addition to this, WO_3 could enter solution by forming a complex with electrolyte anions. Phosphoric acid is known to form complexes with WO_3. To a lesser extent, sulfuric acid may do likewise.

Electrolyte anions are attracted to the surface in the bleached state, and during dynamic bleaching this anion activity is further enhanced. Anions such as SO_4^{2-} may bond to surface molecules forming negative complexes which are swept into solution during coloration. Simple complexes like $[(WO_3)(SO_4^{2-})]^{2-}$ or polymeric complexes like $[(SO_4^{2-}) \cdot (WO_3O_9) \cdot H^+ \cdot (W_3O_9) \cdot (SO_4^{2-})]^{3-}$ could form. Another possibility is a metatungstate isomorph in which SO_6 octahedra are incorporated in place of some WO_3, such as $[H_2^+(WO_3)_8 \cdot (SO_4^{2-})_4]^{6-}$.

Conclusion

Aqueous dissolution and titration results indicate that amorphous WO_3 films (as-deposited) dissolve to form metatungstate or pseudo-metatungstate ions. Moreover, evidence indicates that complex 3-, 6-, or 12-mer ions enter solution directly from the dissolving surface. These results, together with the fact that associative vapor molecules tend to form molecular or semimolecular solids upon condensation, strongly suggest that as-deposited WO_3 films are composed chiefly of trimeric clusters weakly bound to one another. The very open microstructure that would result, along with water-bridge bonds between mole-

cules, can account for the high proton mobilities observed in EC films, but also for the unfortunate rapid dissolution and cycling erosion.

Analysis of evaporated films subjected to oxygen ion bombardment suggests two concepts which may be important to electrochromic development. (*i*) There may exist two distinct amorphous structures, one closer to a molecular solid, the other closer to a random network structure. (*ii*) The restructured (network) film shows decreased colorability, not because it is less permeable to proton flow but because electron injection or transport is inhibited, or noncoloring trapping states are introduced. Further study of bombardment restructuring may provide key information about the effect of microstructure on EC performance.

Cycling erosion can be understood as a natural extension of the dissolution process—voltage enhanced dissolution. Neither impurity side reactions nor any fundamental irreversibility in the proton injection/extraction process need be postulated. In nonaqueous systems, both quiescent dissolution and cycling erosion are slowed because of (*i*) low ionizability and large size of organic molecules such as glycerine and (*ii*) inhibited tungstate ion formation. In these systems, degradation may result from formation of negative complexes with electrolyte anions or from tungstate formation due to H_2O incorporated in the film.

The molecular solid model presented here for electrochromic films may prove to be a fruitful avenue for understanding the nature of coloration in these films. The intervalence transfer model proposed by Crandall and Faughnan (11) may be given physical interpretation by relating phenomenological configuration coordinates to, say, instantaneous configuration of water-bridged W_3O_9 molecules. This would be similar to coloration in charge transfer complexes in solution. Bridging water bonds may be important not only for proton transfer but for electron transfer as well.

Acknowledgments

I wish to thank B. MacIver for performing the ion implants and F. A. Forster, J. Johnson, and D. Eddy for their assistance in the x-ray diffraction studies.

Manuscript submitted Jan. 21, 1980; revised manuscript received July 23, 1980.

Any discussion of this paper will appear in a Discussion Section to be published in the December 1981 JOURNAL. All discussions for the December 1981 Discussion Section should be submitted by Aug. 1, 1981.

Publication costs of this article were assisted by General Motors Research Laboratories.

REFERENCES

1. T. J. Knowles, H. N. Hersh, and W. Kramer, in 19th Electronic Materials Conference of AIME, Cornell, N.Y. (1977).
2. J. P. Randin, in *Ibid.*
3. T. B. Reddy and E. A. Battistelli, in *Ibid.*
4. "Comprehensive Inorganic Chemistry," Vol. 4, A. F. Trotman-Dickenson, Executive Editor, chap. 51, Pergamon Press, England, (1973).
5. H. R. Zeller and H. U. Beyeler, *Appl. Phys.*, **13**, 231 (1977).
6. H. Hashimoto, T. Naiki, M. Mannami, and K. Fujita, in "Structure and Properties of Thin Films," C. A. Neugebauer, Editor, p. 71, John Wiley & Sons, Inc., (1959).
7. J. Berkowitz, W. A. Chupka, and M. G. Inghram, *J. Chem. Phys.*, **27**, 85 (1957).
8. W. Hirschwald and I. N. Stranski, in "Condensation and Evaporation of Solids," E. Rutner, Editor, Gordon and Breach, New York (1964).
9. G. M. Rosenblatt, in "Treatise on Solid State Chemistry," Vol. 6A, Surfaces I, N. B. Hannay, Editor, p. 233, Plenum Press, New York (1976).
10. R. S. Crandall and B. W. Faughnan, *Appl. Phys. Lett.*, **26**, 120 (1975).
11. B. W. Faughnan, R. S. Crandall, and P. M. Heyman, *RCA Rev.*, **36**, 1977 (1975).

SF_6, a Preferable Etchant for Plasma Etching Silicon

K. M. Eisele*

Fraunhofer-Institut für Angewandte Festkörperphysik, D-7800 Freiburg, West Germany

ABSTRACT

SF_6 is a far more selective etchant for silicon than $CF_4 + O_2$ when excited to a plasma discharge. This applies to good advantage in parallel plate reactors where under given conditions of rf power and pressure the etch ratio of silicon to SiO_2 is 30:1 but with CF_4 only 7:1. In contrast to the deposition of carbon in a CF_4 process sulfur has not been found on a silicon surface etched in SF_6. The selectivity of an SF_6 etching process cannot be shifted sufficiently in favor of SiO_2 by adding hydrogen, it can also not be increased much in favor of silicon by adding oxygen. The reaction product is SiF_4. No other silicon compound than SiF_3^+ appeared in the mass spectrum. 1% SF_6 in argon achieves etch rates of more than 100 nm/min with moderate rf energy. SF_6 is also a useful etchant for Si_3N_4 with etch rates of 100 nm/min.

The etching of polysilicon by means of a CF_4 plasma has almost become a standard process in the manufacture of integrated circuits (1). The polysilicon deposited on an SiO_2 layer serves as gate electrode and for interconnections between the active elements, resistors, and bonding pads. The etch rate of a $CF_4 + 4\% O_2$ gas mixture excited to a plasma discharge in a tunnel reactor is selective in favor of silicon over SiO_2 with a ratio of 30:1 (1, 2) so that the SiO_2 is little affected when the time necessary to etch the silicon layer is exceeded by a marginal amount.

Structures of micrometer width are preferably etched in a parallel plate reactor because the anisotropic etching of such a system achieves better definition, less underetching, and better profile control than can be obtained in a tunnel system. Unfortunately, in a parallel plate system the etch ratio $Si:SiO_2$ is reduced to 7:1 and therefore not any longer sufficiently selective.

This fact has given incentive to look for other etchants. Based on earlier experiences in thermally etching silicon surfaces *in situ* before epitaxial growth with SF_6 (3), this gas seemed suitable for trials in plasma etching (10). SF_6 is not inflammable and not toxic.

* Electrochemical Society Active Member.
Key words: plasma etching, silicon, SF_6, selectivity.